Heliyon 10 (2024) e27164

Contents lists available at ScienceDirect

Heliyon

journal homepage: www.cell.com/heliyon

Research article

Curcumin attenuates doxorubicin-induced cardiotoxicity *via* suppressing oxidative Stress, preventing inflammation and apoptosis: Ultrastructural and computational approaches

Ayed A. Shati [a], Refaat A. Eid [b], Attalla F. El-kott [c,d,*], Youssef A. Alqahtani [a], Abdullah S. Shatoor [e], Mohamed Samir Ahmed Zaki [f,g]

[a] *Department of Child Health, College of Medicine, King Khalid University, Abha, Saudi Arabia*
[b] *Department of Pathology, College of Medicine, King Khalid University, Abha, Saudi Arabia*
[c] *Department of Biology, College of Science, King Khalid University, Abha, 61421, Saudi Arabia*
[d] *Department of Zoology, College of Science, Damanhour University, Damanhour, 22511, Egypt*
[e] *Department of Internal Medicine, College of Medicine, King Khalid University, Abha, Saudi Arabia*
[f] *Department of Anatomy, College of Medicine, King Khalid University, Abha, Saudi Arabia*
[g] *Department of Histology and Cell Biology, College of Medicine, Zagazig University, Zagazig, Egypt*

ARTICLE INFO

Keywords:
Doxorubicin
Curcumin
Oxidative stress
Heart injury

ABSTRACT

Currently, doxorubicin (DOX) is one of the medications commonly used in chemotherapy to treat different types of tumors.Nonetheless, despite being effective in multiple tumors, yet its use is limited owing to its cytotoxic effects, the therapeutic use of DOX has been limited. This work aimed to explore whether curcumin (CMN) can prevents DOX-induced cardiotoxicity in rats. Four groups of rats were created, with the first functioning as a control, while the second group received CMN. DOX alone was administered to the third group, whereas CMN and DOX were administered to the fourth group. Lipid peroxidation assessed as Malondialdehyde (MDA), aspartate aminotransferase (AST), alanine aminotransferase (ALT), oxidative stress markers as catalase (CAT), superoxide dismutase (SOD), and inflammatory markers as tumor necrosis factor-alpha (TNF-α) in heart homogenates, each one was assessed. Heart specimens was investigated histologically and ultrastructurally. Increased, AST, and ALT serum levels, increased MDA levels, decreased SOD and CAT levels, and increased TNF-α concentrations in heart homogenates were all signs of DOX-induced myocardial injury. Histological and ultrastructural examinations revealed vacuoles and larger, swollen mitochondria in the cytoplasm. Furthermore, DOX caused significant changes in the myocardium, most notably nuclei disintegration, myofibrillar loss, and myocyte vacuolization. Using CMN with DOX reduced the harmful consequences of DOX on the myocardium by returning the increased AST and ALT levels to their original levels as compared to the control and reducing them. In cardiac tissue, CMN significantly increased the concentrations of SOD and CAT and significantly decreased the concentrations of MDA and TNF-α. Biochemical and histological studies have demonstrated that CMN has a heart-protective effect that might be related to its antioxidant and anti-inflammatory capabilities.

* Corresponding author. Department of Biology, College of Science, King Khalid University, Abha, Saudi Arabia.
E-mail addresses: ashati@kku.edu.sa (A.A. Shati), raeid@kku.edu.sa (R.A. Eid), elkottaf@yahoo.com (A.F. El-kott), Yal-qahtani@kku.edu.sa (Y.A. Alqahtani), asshalghamdi@yahoo.com (A.S. Shatoor), mszaki@kku.edu.sa, mszaki1957@gmail.com (M.S. Ahmed Zaki).

https://doi.org/10.1016/j.heliyon.2024.e27164
Received 12 June 2023; Received in revised form 24 February 2024; Accepted 26 February 2024
Available online 27 February 2024

1. Introduction

Chemotherapeutic agents with anthracyclines may interact with DNA and biological components [1]. Multiple cancer therapeutic drugs are frequently used to treat various tumors. Tolerance to medication, and other serious adverse effects reduce the effectiveness of these drugs, which could result in increased mortality rates or reduced quality of life in cancer patients [2]. Cardiac toxicity hazardous to human health [3]. Despite being frequently hematological tumors, the anthracycline DOX is limited because of its toxicity to organs [4,5]. Researchers have shown that cumulative dose of DOX can abruptly and persistently cause cardiac muscle fiber injury that may be reversible through multiple mechanisms such as nucleic acid suppression which interfere with macromolecular biosynthesis by embedding into the helix of DNA double strands., reactive oxygen species generation, and mitochondrial dysfunction. This has sparked interest in the domain of studying cardiomyopathy caused by chemotherapy [6]. More than 25% of cancer patients receiving DOX may experience dose-dependent and cumulative myocardial injury leading to congestive heart failure, cardiomyopathy or arrhythmia [7], might be related to myocardial fibrosis, progressive ventricular distension, systolic failure., and mitochondrial ballooning (sign of heart damages) [8–10].

Once the production of reactive oxygen species (ROS) reaches its peak, it overcomes the antioxidant defenses generated by the cell, creating an intracellular condition known as oxidative stress that is inherently risky for the cell's constituent elements. It is widely believed that account for the toxicity of DOX in cardiac muscle fibers [6]. Factors that contribute to both apoptosis and necrosis [11]. It has been postulated that DOX treatment on a regular basis lowers antioxidant levels while concurrently raising lipid peroxidation level, leading to the development of cardiomyopathy. Oxidative damage level Two of the mechanisms by which DOX induces cardiac myocyte damage are increased apoptosis and aggravated inflammation.

There are several approaches that have been proposed to avoid the risks of DOX-induced cardiotoxicity. According to a recent article published in Cardiovascular Toxicology, some of the proposed approaches include targeting mitochondria to improve metabolic function, inhibiting inflammatory cytokines, and reducing oxidative stress pathways [12]CMN has been demonstrated to be an effective drug due to its established antioxidant action [13]. However, CMN's poor solubility and rapid systemic elimination restrict its application in healthcare situations. This problem has been resolved, the nano formulation of CMN the physicochemical properties essential for its efficacy [14]. Turmeric (Curcuma longa), a naturally occurring plant in Southeast Asia, contains CMN. Interestingly, CMN has a heart-protective effect when administered in conjunction with DOX, might be attributed to the anti-oxidative activity of CMN-derived linoleate "a polyunsaturated fatty acid" that is capable of inhibiting lipid peroxidation through forming fatty acid radicals and acting as ROS scavenger [15].However, CMN treatment may aid in protecting the myocardium, where biomarkers such as aspartate aminotransferase (AST), alanine aminotransferase (ALT), were significantly decreased, CAT and SOD levels increased, whereas MDA levels often improved [16]. Antioxidants such as CAT, SOD, and MDA are responsible for inhibiting and reducing damage caused by free radicals in cells [17]. Reducing the degree of lipid peroxidation in heart myocytes caused by both CMN and DOX suggests that CMN may have some cardioprotective characteristics, further supporting the idea that CMN has the capacity to decrease the negative consequences of DOX [18]. This study focused on how oxidative stress affects the heart by examining the potential of CMN in preventing DOX-induced cardiac myocyte damage.

2. Materials and methods

2.1. Drugs and chemicals

DOX (Sigma-Aldrich in St. Louis, MO (USA).

Powdered Curcuma longa (turmeric) was used to make CMX (CAS Number: 458-37-7; Sigma). Alanine Transaminase Activity Assay Kit (Colorimetric/Fluorometric) (ab105134).

Aspartate Aminotransferase Activity Assay Kit (ab105135).

MDA (Assay Kit) (Sigma-Aldrich in St. Louis, MO (USA)).

Abcam provided the CAT (ab83464 Assay Kit) and SOD (ab65354 Assay Kit). TNF-α: derived from Santa Cruz Biotechnology Inc., Dallas, Texas (sc-28318).

Serum CK-MB (Catalogue No.: MBS2515061) and troponin (Catalogue No.: MBS038739) were determined using specific ELISA kits supplied by MyBioSource (San Diego, USA).

2.2. Experimental design and animals

For this investigation, King Khalid University College of Medicine contributed twenty-four male Wistar albino rats. Each rat weighed 200 ± 50 g and was given free access to tap water and a pure diet, AIN-93 M (Research Diets, NJ, USA). Four groups of rats were created, with each group receiving adequate care to reduce pain or suffering. In addition, the welfare of the experimental rats was carefully monitored, and appropriate measures were taken to ensure maximum welfare. The research ethics committee at King Khalid University approved the experimental approach, which was associated with the implementation to be used and managed by laboratory animals from the National Institutes of Health (NIH Publication No. 85-23, updated 1985). Following acclimatization to the laboratory environment for 2 weeks, the rats were randomly assigned into four groups of six rats each. The groups formed can be described as follows.

Group 1. (Control): Rats were given oral corn oil by gavage for 15 days and one intraperitoneal injection of saline solution (0.9%

NaCl) on the 10th day.

Group 2. (CMN) got CMN CMN (100 mg/kg body weight) for 15 days. The CMN dosage was chosen in accordance with Yu et al. [19].

Group 3. (DOX induced cardiotoxicity): Rats were orally administered corn oil orally for 10 days. On the11th day, the rats received an intraperitoneal injection of DOX (20 mg/kg bw), followed by five consecutive days of daily oral gavage administration of corn oil. Lv et al. [20] approach was used to calculate the DOX dosage.

Group 4. (DOX + CMN-induced): Rats administered oral gavage doses of CMN (100 mg/kg body weight) for ten days. After receiving an intraperitoneal dose of DOX (20 mg/kg bw) on the eleventh day, rats were administered CMN (100 mg/kg bw) orally every day for five days.

The crushed plant solid Curcuma longa (turmeric) sample wass subjected to a solvent, usually acetone, methanol, ethanol, or isopropanol, in the first stage of this method. The solute of interest is then dissolved in the solvent and freed from the solid matrix in the second stage. Gathering the solute is the final stage [21].

2.3. Estimation of oxidative stress and TNF-α markers

. Blood samples were collected into Eppendorf tubes. After allowing it to coagulate in the oven for 15 min, it was centrifuged at 5000 rpm for 20 min to separate the serum. The ALT and AST biomarkers were measured using collected serum through enzymatic assays. These assays are based on the principle that AST and ALT catalyze the transfer of amino groups from aspartate and alanine, respectively, to alpha-ketoglutarate, forming oxaloacetate and pyruvate, respectively. The resulting oxaloacetate and pyruvate are then detected by measuring the absorbance of the NADH produced in the reaction [22]. A piece per heart tissue was taken to generate a homogenate, which was then used to measure the levels of CAT [23], SOD [24]and MDA [24,25]. The levels of TNF-α immune expression in the cardiac section were investigated [26]. To assess TNF-α, primary antibodies against TNF-α were applied to sections and incubated at a concentration of 1:200 using ImageJ software (version 1.46a, NIH, Bethesda, MD, USA).

2.4. Determination of serum troponin and creatine kinase-MB (CK-MB)

Serum CK-MB and troponin were determined using specific ELISA kits supplied by MyBioSource (San Diego, USA) according to manufacturer's instructions [27].

2.5. Histopathological examination of heart tissue

Heart samples were extracted from rats in each group. Ten percent neutral buffered formalin was used to fix the specimen prior to processing [28]. Hematoxylin and eosin (H&E)-prepared sections of five μm thickness were used and sequentially stained in Masson's trichrome for 5 min each with solutions of iron hematoxylin, acid Ponceau fuchsin, and aniline blue. Using an Olympus BX50 light microscope (Tokyo, Japan), histopathological analysis was performed [29].

2.6. Ultrastructural examination of heart tissue

For 24 h, small pieces were fixed in 2.5% glutaraldehyde and then rinsed in phosphate buffer (0.1 M, PH 7.4). For 2 h, post-fixation was performed in 1% osmium tetroxide buffered with phosphate buffer to remove the extra fixative, dehydrated through increasing ethanol concentrations, and cleared in propylene oxide. The samples were packaged inside gelatin capsules filled with Araldite 502. The capsules were polymerized by heating them to 60 °C.

For orientation and observation, toluidine blue-stained semi-thin sections of around 1-μm thickness were prepared. Using an ultramicrotome, extremely thin sections were created and then gathered on uncoated copper grids. A JEOL transmission electron microscope (JEM-1011, JEOL Co., Tokyo, Japan) was used to analyze and snap photographs of the sections after they had been double-stained with lead citrate and uranyl acetate [30]. Understanding the subcellular elements of cells and tissues requires first quantifying the organelles in TEM pictures. The National Institutes of Health originally developed ImageJ, an open-source program that may be used to measure organelles in TEM images. The program may be used to examine the mitochondrial/endoplasmic reticulum (ER) interaction and measure parameters including mitochondrial length, width, area, and circularity [31].

2.7. Statistical analysis

Data were analyzed using the SPSS Software program version 29 (IBM SPSS Statistics for Windows, Armonk, NY: IBM Corp). Continuous variables are presented as the mean ± SD (standard deviation). The IBM Social Sciences Statistical Package (SPSS) program was used to assess the statistical significance of differences among groups using one-way analysis of variance (ANOVA) and Duncan's post hoc test. Statistical significance was defined as $p < 0.05$.

3. Results

3.1. Effect of DOX and CMN on the rat mortality rate

DOX treatment increased the mortality rate (2 out of 6) compared with that for control animals. Co-treatment of rat with DOX + CMN significantly decreased the rat mortality rate (0 out of 6) compared with DOX treatment alone. No mortality was recorded in the control group or the CMN-treatment group during the study period.

3.2. Body weight and heart weight to body weight ratio

The body weight and heart weight to body weight ratio in DOX group were significantly increased compared with control rats. The heart weight, body weight and ratio of heart weight to body weight in DOX plus CMN group was significantly decreased compared with DOX induced (Table 1).

3.3. Biochemical results

3.3.1. Lipid peroxidation (MDA) and antioxidant enzyme levels

As evidenced by the increase in cardiac MDA, AST, and ALT srum levels compared to control and CMN groups, it has been observed that DOX induces lipid peroxidation. MDA, AST, and ALT levels were significantly lower in DOX- and CMN-treated rats than in those exposed to DOX (Fig. 1A, B, and 1C). The cardiac CAT and SOD levels were lower DOX-treated groups than in the control and CMN groups. DOX plus CMN therapy improved the reduction of SOD and CAT compared with the levels observed in animals administered DOX (Fig. 2A and B).

3.3.2. Troponin and creatine kinase-MB (CK-MB) levels

In the present study, DOX induced myocardial damages in rats was evidenced by higher levels of serum troponin and CK-MB levels. Decreased levels of these biochemical markers were observed in CMN cotreated with DOX treated rats compared to DOX treated control group (Fig. 3A and B).

3.3.3. Levels of pro-inflammatory cytokine TNF-α

TNF-α concentrations were assessed in the cardiac tissues of all the groups. DOX-treated rats had significantly higher TNF-α levels in this tissue than in the control and CMN groups. However, according to the levels observed in DOX-treated rats, DOX in conjunction with CMN supplementation mitigated the damage caused by TNF-α (Fig. 4).

3.4. Histological and ultrastructural results

3.4.1. Control and CMN groups

The characteristic histological structure of cardiac muscle fibers was observed in H&E-stained sections; they were arranged in an anastomosing, branching pattern, with oval nuclei and an acidophilic sarcoplasm in the middle (Fig. 5A and Table 1). Sections that had been stained with Masson's trichrome revealed a few collagen fibers enclosing the cardiac muscle bundles (Fig. 6A and Table 1).

Ultrastructural investigation was performed on ultrathin sections, which revealed an abundance of cytoplasm comprising many healthy myofibrils with myocardial striations in their natural form, regularly spaced sarcomeres, and obvious bands (Z and H) with well-preserved mitochondrial integrity. A centralized euchromatic nucleus with regularly dispersed chromatin and intact nuclear-enveloped membrane was observed. (Fig. 6 A, B, and Table 1). Desmosomes, gap junctions, and intercalated discs with distinctive fascial adhesions were also observed (Fig. 8 A and Table 1). Simple squamous endothelial cells formed capillaries by overlapping the vascular lumen (Fig. 9 A and Table 2).

3.4.2. DOX treated group

H&E-stained sections showed pronounced fibrinolysis of splitting wavy, widely dispersed, and disordered heart muscle fibers with pyknotic nuclei, congested blood capillaries, and edema within the myocardium (Fig. 5 B&C and Table 1). Masson's trichrome stain

Table 1
Effect of curcumin (CMN) on body weight, and heart weight to body weight (HW/BW) ratio in doxorubicin (DOX) induced cardiotoxicity in rats.
[Values are mean ± SE from 6 rats].

Treatment groups	Body weight (g)	HW/BW ratio ($\times 10^{-3}$)
Control	272.33 ± 09.667	32.245
CMN-induced	253.49 ± 15.819	34.3124
DOX induced	263.23 ± 6.269*	63.71
DOX plus CMN-induced	201.72 ± 4.163$^{\&}$	39.954

Data are expressed as means ± S.D. *$p < 0.05$ compared with control. $^{\&}p < 0.05$ compared with DOX group.

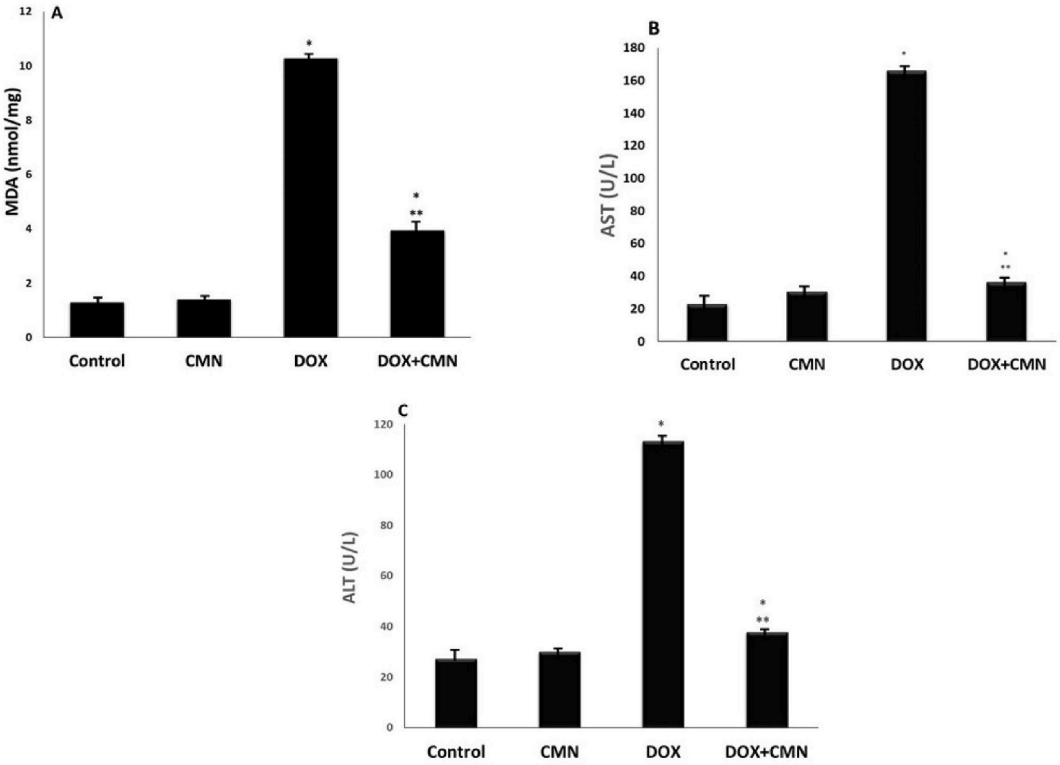

Fig. 1. Rats exposed to DOX had biochemical indices that significantly increased the levels of MDA (A), AST (B), and ALT (C) between the four research groups which are considered clinical indicators of oxidative stress. The increased ALT, AST, and MDA levels were significantly reduced when CMN was added to the DOX group.
The results represent the mean (±SD), n = 6, *p < 0.05 in comparison to controls, and ***p < 0.05 contrary to DOX group.

revealed that there had been a significant accumulation of collagen fibers (Fig. 6 B&C and Table 1).

Ultrastructural analysis revealed oversized mitochondria with disorderly cristae, flocculent density accumulation, and abnormalities within the mitochondrial outer membrane in addition to damaged myofibrils and disordered Z and H muscle bands. Additionally, it was possible to observe the disassembling of the outer nuclear layer, clumped chromatin dispersed randomly throughout the nuclei, and demarcated spaces within the nuclei (Fig. 7 C&D). Intercalated discs that were damaged with obvious disruption of their components, such as desmosomes, gap junctions (Nexus), and adherent fascia (Fig. 8 B and Table 1), as well as distorted capillaries with malformed endothelial cells (Fig. 9 B and Table 2).

3.4.3. DOX plus CMN group

The normal myocardial structure was only restored in H&E-stained sections, and vasculature congestion was observed (Fig. 4 D). Slightly accumulated collagen fibers were visible by Masson's trichrome staining (Fig. 6 D).

Ultrastructural analysis revealed a typical, integrity-preserving architecture coupled with a nucleus with a proper chromatin structure and nuclear envelope, intact mitochondria, and a striated appearance made up of bands (Z and H) (Fig. 6 E and F). Intact intercalated discs formed of fascial adherent, desmosome, and gap (nexus) junctions (Fig. 8C), and the preserved capillaries surrounded by normal endothelial cells were evaluated (Fig. 9C).

4. Discussion

About 30% of cancer patients experience DOX-induced cardiac toxicity, which is often detected days after the last DOX treatment as cumulative effect [19]. To some extent, the present investigation reveals a clear understanding of the mechanism of DOX-induced cardiac muscle fibers. However, a sizable body of data indicates that oxygen-free radical production can cause lipid peroxidation and consequent cell injury. Rats administered DOX had significantly higher MDA levels in their cardiac tissues, as observed by the investigators, indicating enhanced lipid peroxidation. Previous studies in rats have demonstrated that elevated oxidative stress and antioxidant deficiencies may be the etiology of heart tissue injury [32].

This study revealed that DOX caused substantial oxidative damage in the cardiac tissue. Following severe tissue injury, transaminases such as ALT and AST are released. As both are abundant in the heart muscle (particularly AST), it is likely that their elevated levels signify myocardial injury. AST seum level was much higher in DOX-treated rats than in control and CMN rats, indicating serious

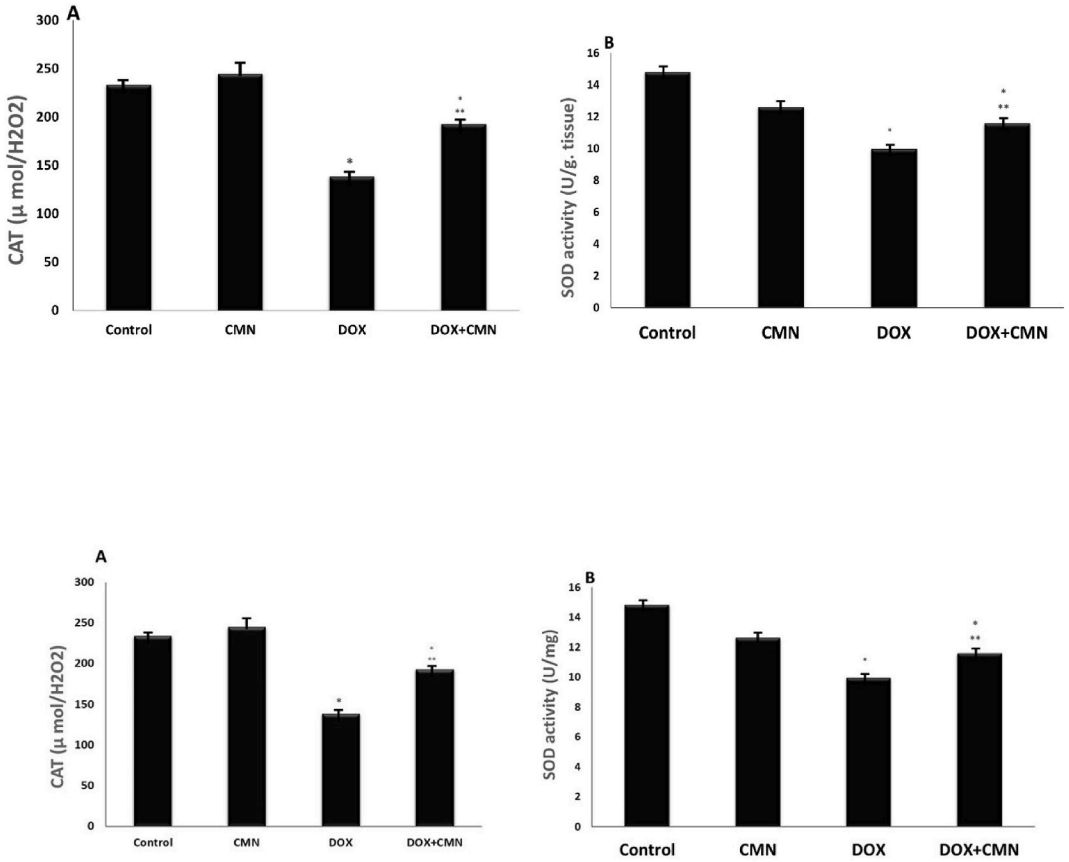

Fig. 2. Showed found the DOX group's CAT (A)and SOD (B)activity was lower than that of the control group. The DOX group's CAT and SOD activity significantly increased after taking CMN.
The observations are the mean (±SD); n = 6. *p < 0.05 compared to the controls; ***p < 0.05 in contrary to the DOX group.

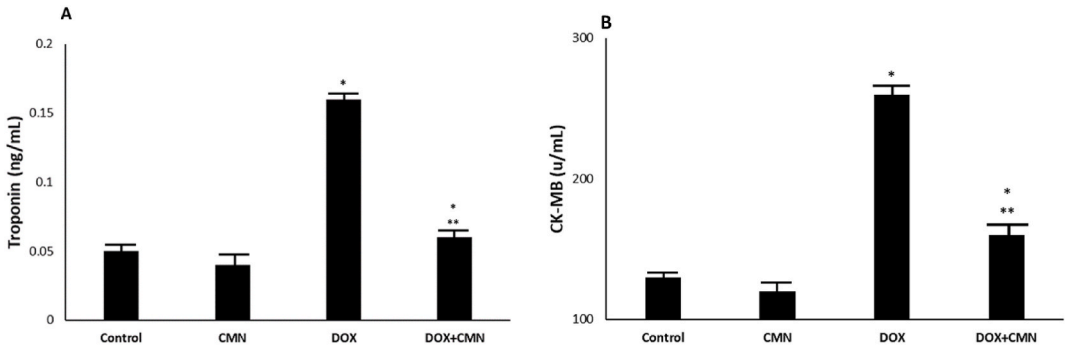

Fig. 3. CK-MB and troponin levels were significantly higher in DOX treated group than those of control group. These levels were significantly lower in CMN cotreated with DOX in comparison to those of DOX treated group.
The results are the mean (±SD), n = 6. *p < 0.05 compared to the controls, and ***p < 0.05 in comparison to the DOX group.

cardiac injury. This outcome is consistent with [29]. Following DOX treatments, there was a considerable increase in the concentrations of the heart damage marker, AST enzyme [33–35].

However, compared with the control and CMN groups, myocardial CAT levels was significantly reduced in this study. Rats given DOX exhibit an increase in cardiovascular oxidative stress, cellular membrane damage, and a significant drop in the antioxidant CAT [36].

Throughout the study, rats administered DOX showed decreased SOD and CAT levels, supporting the relationship between oxidative stress and cardiac damage. There is no disputing the fact that SOD inhibits the formation of OH radicals by converting O^2-

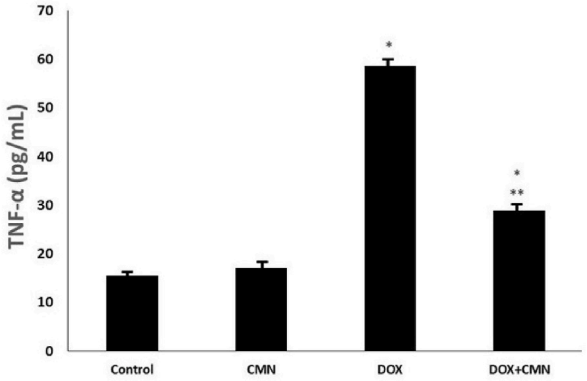

Fig. 4. Rats exposed to DOX showed significantly increased levels of pro-inflammatory biomarker TNF-α in the studded groups. The DOX group's TNF-α activity significantly reduced after taking CMN.
The results are the mean (±SD), n = 6. *p < 0.05 compared to the controls, and ***p < 0.05 in comparison to the DOX group.

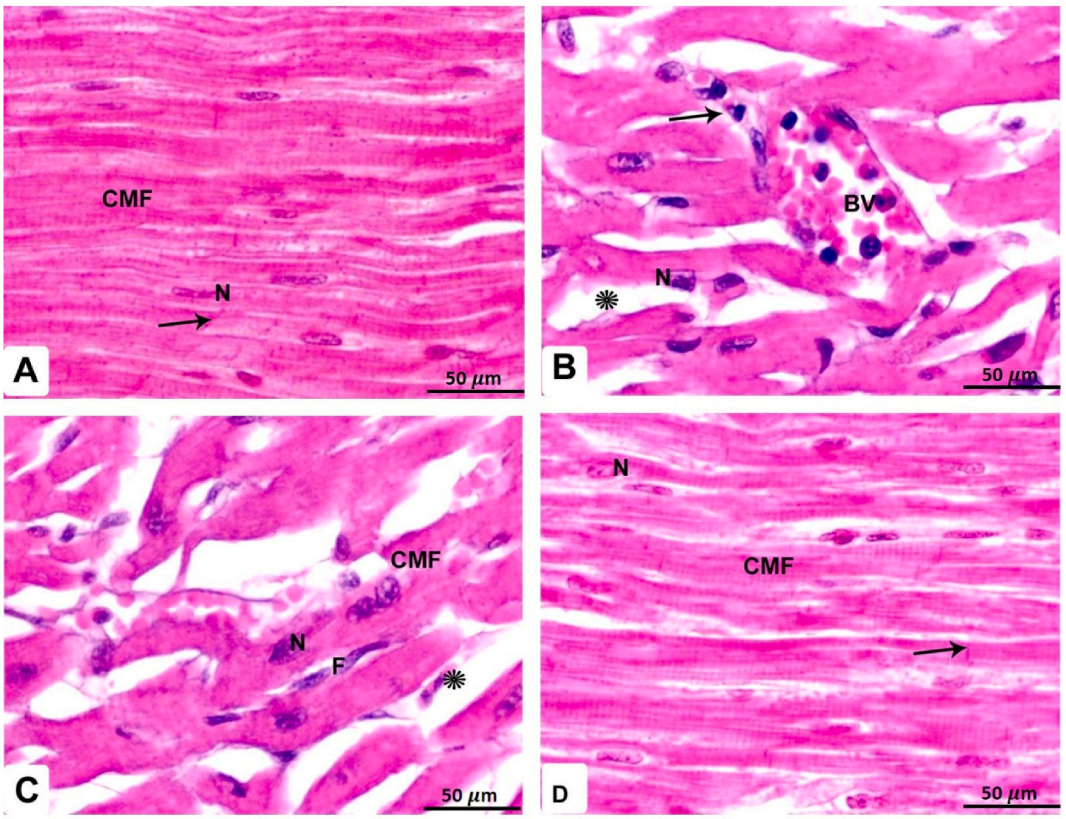

Fig. 5. Displays photomicrographs of illustrated heart sections stained with H&E.
(Scale bar: 50 μm)
A: Heart tissues from the controls and CMN rats: branching cardiac muscle fibers (CMF) with acidophilic sarcoplasm, an oval nucleus (N) situated in the center, and intercalated discs are visible (arrow).
B: DOX intoxicated hearts showing cardiac muscle fibers disorganization with pyknotic nuclei (N), congested blood vessels (BV), perivascular fibroblasts (arrow), and intramyocardial edema (*).
C: DOX intoxicated hearts showing prominent fibrinolysis of disorganized splitting wavy cardiac muscle fibers (CMF), which are widely spaced with pyknotic nuclei (N) and multiple fibroblasts (F) in between.
D: DOX plus CMN group showing more or less complete restoration of the normal histological structure of cardiac muscle fibers (CMF) with a central oval nucleus (N), blood capillaries, and normal intercalated discs are shown in the image.

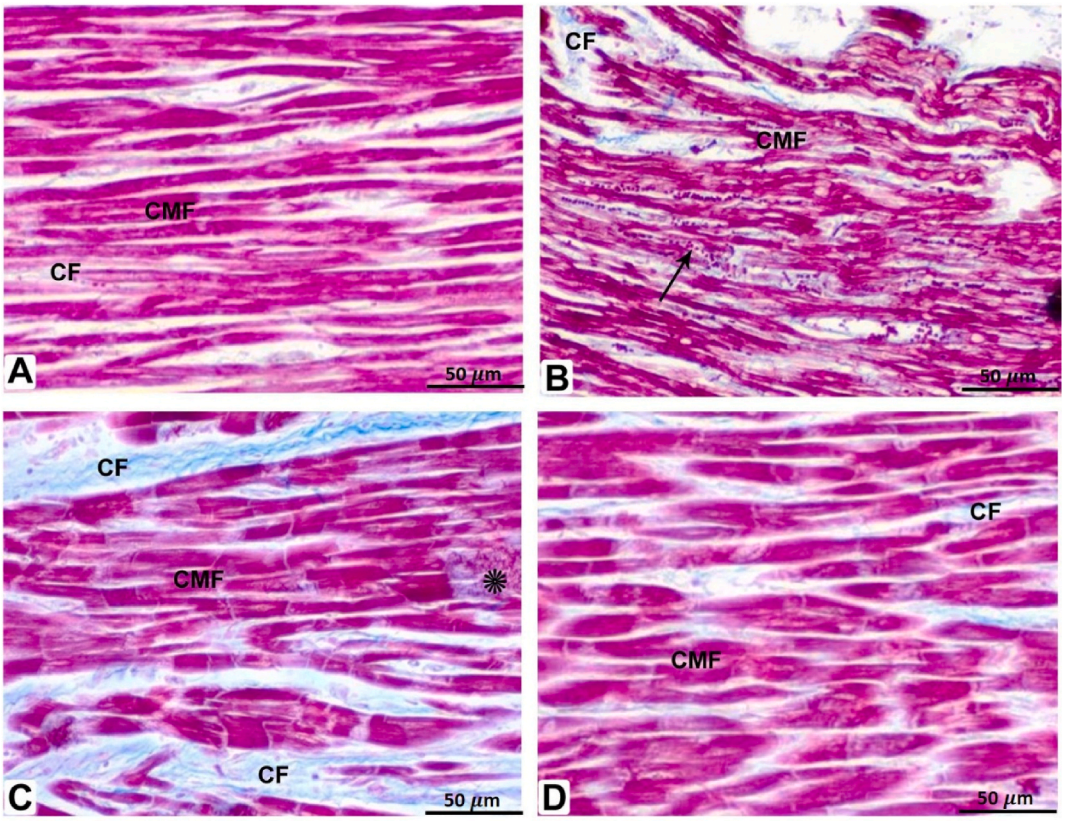

Fig. 6. Masson's trichrome-stained heart section photomicrographs
(Scale bar: 50 μm)
A: Cardiac tissues from the controls and CMN rats are exhibited branched cardiac muscle fibers (CMF) with a minimal amount of collagen fibers (CF) in between.
B: DOX-intoxicated hearts with disorganized splitting wavy cardiac muscle fibers (CMF) that are widely spaced, interstitial hemorrhage (arrow), and collagen fiber accumulation (CF).
C: DOX-intoxicated hearts with disorganized cardiac muscle fibers (CMF) that are widely spaced with large amounts of collagen (CF) fiber accumulation and focal necrosis (*).
D: DOX plus CMN group showing nearly more or less complete restoration of the regular morphology of cardiac muscle fibers (CMF) with mild amounts of collagen fibers (CF).

Table 2
Demonstrating the percentages scoring system of Cardiac histopathological & ultrastructural features of all groups of rats.

No	Cardiac Structures		Percentages			
			Control group	CMN group	DOX group	DOX plus CMN group
1	**Histopathological Analysis**	**Muscle fibers**	**0–1 %**	**1–2 %**	**24–27 %**	**1–4 %**
		Branching cardiac fibers	**0–1 %**	**2–3 %**	**35–40 %**	**2–3%**
		Connective tissues	**0–1 %**	**0–2 %**	**55–58 %**	**1–2 %**
		Central nuclei	**0–1 %**	**0–1 %**	**25–28 %**	**2–3 %**
		Cross striations	**0–1 %**	**1–2 %**	**35–41 %**	**2–3 %**
2	**Ultrastructural Analysis**	**Intercalated discs**	**0–1 %**	**1–2 %**	**35–40 %**	**1–4 %**
		• Fascia adherence	**0–1 %**	**1–2 %**	**24–27 %**	**1–5%**
		• Macula adherent	**0–1 %**	**1–2 %**	**11–18 %**	**1–7 %**
		• Gap junctions	**0–1 %**	**1–2 %**	**35–40 %**	**2–3 %**
		Cardiomyocytes	**0–1 %**	**1–2 %**	**44–58 %**	**1–2 %**
		Myofibrils	**0–1 %**	**1–2 %**	**55–58 %**	**1–4 %**
		Z and H bands	**0–1 %**	**1–2 %**	**50–61 %**	**0–1 %**
		Mitochondria	**0–1 %**	**1–2 %**	**45–50 %**	**1–2 %**
		Blood capillaries	**0–1 %**	**1–2 %**	**25–28 %**	**1–4 %**
		Interstitial area	**0–1 %**	**1–2 %**	**46–57 %**	**2–3 %**
		Collagen fibers	**0–1 %**	**1–2 %**	**54–66 %**	**2–3 %**

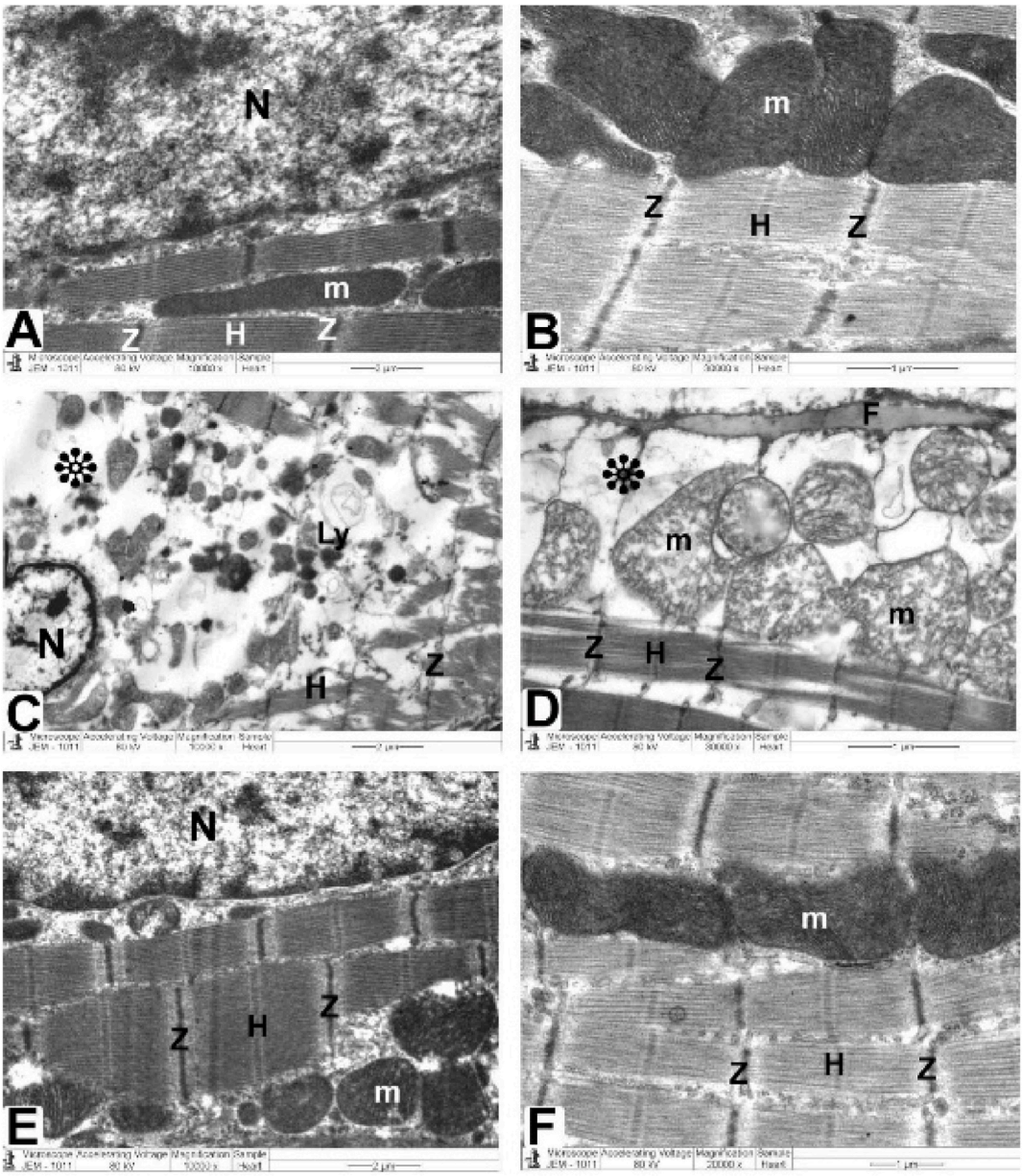

Fig. 7. Heart architecture as shown in TEM images from all groups.
Control and CMN groups (Fig. 6A and B) exhibit abundant cytoplasm packed with healthier myofibrils with normal myocardial striations architecture with regularly arranged sarcomeres and obvious bands (Z and H) with mitochondrial (m) integrity that has been preserved and arranged in rows between. There is a nuclear envelope and a central euchromatic nucleus (N) with properly dispersed chromatin.
DOX group (Fig. 6C and D) shows swelling and degenerated mitochondria mitochondria (m) with disordered cristae, flocculent density deposits, outer mitochondrial membrane abnormalities, disturbed myofibrils, with disarrangement of muscle bands (Z and H). Nuclei (N) with minimal heterochromatin material distributed within the nucleoplasm and along the nuclear envelope, and there are noticeable spaces (*) inside the nuclei.
DOX plus the CMN group (Fig. 6E and F) demonstrates typical structure with a striated pattern of distinct bands (Z and H) and preserved integrity, the nucleus (N) with appropriate chromatin organization and the nuclear envelop, and preserved mitochondria (m).

radicals to H_2O_2, [37]. DOX treatment promotes the production of proinflammatory cytokines such as TNF-α [38,39]. TNF alpha is a type of cytokine that is released when the body detects harmful stimuli such as infections or injuries. It helps to start the inflammatory response by attracting and activating immune cells to fight the invaders [40].

The vehicle-treated rat hearts used in the current study had a normal appearance and exhibited no morphological alterations. The size, shape, and structure of the heart muscle fibers were uniform. All DOX-injected rats developed cardiomyopathy, as evidenced by a condition in which the cytoplasm contained vacuoles and swollen inflated mitochondria. Additionally, DOX caused significant

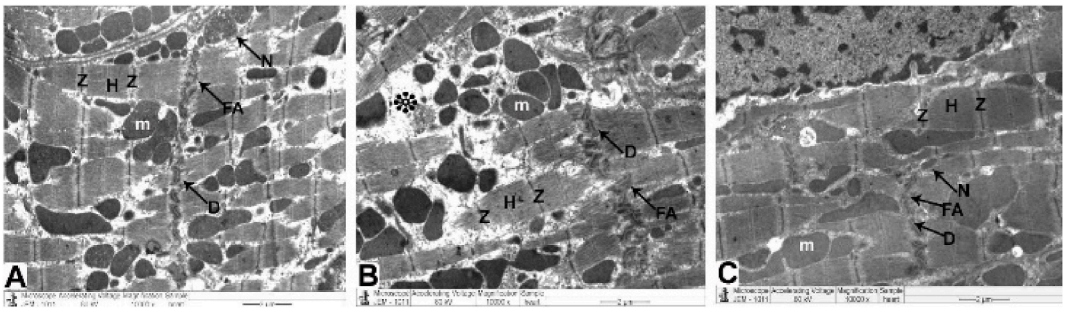

Fig. 8. TEM micrographs of Intercalated disc attained from all groups
The control and CMN groups (Fig. 7A) demonstrate a normal cardiomyocyte with a striated pattern with obvious bands (Z and H), maintained mitochondria, and an abundance of cytoplasm and myofibrils (m). Additionally, intercalated discs comprise desmosomes (D), fascia adherent (FA) junctions, and gap junctions (nexus) (N).
DOX group (Fig. 7. B): demonstrate pleomorphic mitochondria, disordered myofibril cytoplasm, and muscular band disorder (Z and H) (m). Fascia adherent (FA), desmosomes (D), and gap junctions (Nexus) (N) are among the components of intercalated discs that are disturbed.
DOX plus CMN group (Fig. 7C) reveals undamaged myofibrils, a striated pattern of clear bands (Z and H), healthy mitochondria (m), and typical intercalated discs (fascia adherent (FA), desmosomes (D), and gap junctions (N)) are also assessed.

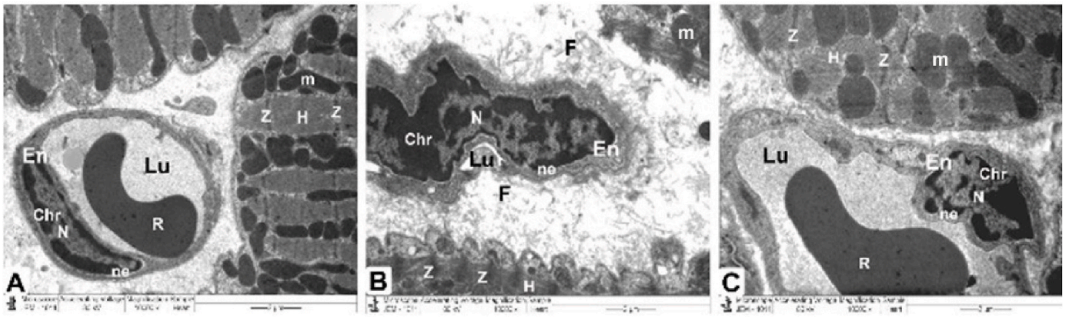

Fig. 9. TEM micrographs of the mitochondria, Z and H band, and endothelial cells from all groups.
The control and CMN groups (Fig. 8 A) Healthful myofibrils with typical myocardial striations, and distinct bands (Z and H) can be found in a cytoplasm that is densely packed. Endothelial cells (En) and their nuclei (N) with regularly distributed heterochromatin (Chr) and regular nuclear envelope (ne), which overlap to form the vascular lumen (Lu), are seen in capillaries, along with preserved mitochondrial integrity (m).
DOX group (Fig. 8. B): reveals enlarged mitochondria (m), deformed capillaries with damaged endothelial cells (En) that create a vascular lumen (Lu) and disrupted myofibrils with altered muscle bands (Z and H). with a disintegrated irregular nucleus (N) with disrupted heterochromatin (Chr) and irregular nuclear envelope (ne). Note that collagen fibrils (CF) are being deposited.
DOX plus CMN group (Fig. 8. C): demonstrates the typical architecture of cardiac muscle fibers, which is kept intact and has a striated pattern of distinct bands (Z and H), preserved mitochondria (m), and intact capillaries with healthy endothelial cells (En) that form the vascular lumen (Lu) and its more or less health nucleus (N) with regularly distributed heterochromatin (Chr) and some irregularity of its nuclear envelope (ne).

alterations in the myocardium, which manifested mostly as cardiac muscle fiber degradation, vacuolization, and fragmentation of nuclei by reducing the activity of topoisomerase and creating ROS [41].

Electron microscopy revealed heavily damaged pleomorphic, disorganized mitochondria with fragmented cristae. Different studies [42–44] attributed these changes to the alteration of calcium homeostasis and blockage of Na+/K + ATPase, which results in intracellular sodium accumulation that causes mitochondrial swelling. High mitochondrial density and heart muscle fibers contain minimal amounts of enzymatic antioxidants that have a significant effect on this mechanism. Additionally, DOX can impair mitochondrial membrane potential, creating alterations in the way mitochondria manage calcium and modify ATP synthesis, all of which eventually result in mitochondrial malfunction, which initiates cellular apoptosis and cardiomyopathy [45].

DOX is frequently used to generate [46,47]. Myocardial infarction, ischemia/reperfusion damage, and hypertrophy are disorders in which cardiac function deteriorates, and have been linked to oxidative stress. High ROS levels cause cellular damage, including necrosis and apoptosis [48]. Through disruption of the balance between the cellular antioxidant system and ROS production, DOX creates an oxidative stress status that is closely related to DOX-associated cardiac alterations [49]. In this study, collagen fibers were abundant in the myocardium and interstitial tissue of DOX-treated animals in comparison to the control group. Neurohumoral substances like fibroblast growth factor, which are both locally and systemically generated, promote collagen synthesis and fibroblast proliferation [50].

CMN's antioxidant-sparing activity enhanced the antioxidant status and consequently mitigated cardiac injury. There may be one or more interactions in the CMN antioxidant pathway, such as free radical scavenging [51], preventing oxidizing enzymes, such as

cytochrome P450 [52], oxygen quenching, reducing its availability for oxidative reactions, avoiding consequences, and neutralizing the oxidative characteristics of metal ions [53]. In this approach, CMN successfully reduced tissue damage by restoring the antioxidant status and reducing oxidative stress.

The present findings imply that treatment with CMN may prevent myocardial injury, since rats treated with CMN plus DOX had lower levels of AST and ALT compared to those in the DOX-only group. These data indicate that CMN maintains the cardiac muscle fibers' natural architectural and structural consistency, which can be explained by CMN's ability to stabilize membranes, as shown by the near-normal AST and ALT enzymatic activity [5].

In this study, CMN stopped DOX-triggered alterations in MDA with a reduction in lipid peroxidation. The cardiac tissue of the group treated with CMN plus DOX showed higher SOD and CAT activities. Some studies have indicated that CMN exerts a protective effect [54]. Following CMN's administration with DOX, on the other hand, significantly reduced these cardiac abnormalities, demonstrating CMN's benefits to heart health [55].

In the present study, DOX induced myocardial damages in rats was evidenced by higher levels of serum troponin and CK-MB levels. Decreased levels of these biochemical markers were observed in CMN cotreated with DOX treated rats compared to DOX treated control group. Therefore, it has been observed that CMN has cardioprotective effects which are most likely due to antioxidant and free radical scavenging activity [56].

Co-treatment of CMN with DOX reduced TNF-α immunological expression in cardiac tissue, highlighting the anti-inflammatory potential of CMN [49].

In order to lessen oxidative stress—which was seen in the histological examination—and to restore the normal structure of the cardiac tissues in the treated rat models, DOX and CMN were used in the procedure. These histological changes could be related to the polyunsaturated fatty acid linoleate, which is produced from CMN, and its antioxidative properties, which can scavenge ROS and generate fatty acid radicals to prevent lipid peroxidation [14], and enhancing heart-protective mitochondrial respiratory chain enzymes [57]. According to histopathological assessment, DOX-induced heart damage was reduced in the CMN treatment group.

5. Conclusion

By administering DOX along with bioactive dietary supplements like CMN, the effect of DOX can be lessened. Consequently, administering CMN as an adjuvant medication may serve as an antioxidant-based preventative or curative strategy to treat cardiac muscle fibers affected by DOX. The study was limited by the fact that the rats were cancer-free, while DOX is typically given to treat cancer after it has manifested in humans or other animals. As a result, the results of this investigation may have been impacted by cancer and its side effects, such as inflammation.

CRediT authorship contribution statement

Ayed A. Shati: Writing – review & editing, Writing – original draft, Visualization, Validation, Supervision, Software, Resources, Project administration, Methodology, Investigation, Funding acquisition, Formal analysis, Data curation, Conceptualization. **Refaat A. Eid:** Writing – review & editing, Writing – original draft, Visualization, Validation, Supervision, Software, Resources, Project administration, Methodology, Investigation, Formal analysis, Data curation, Conceptualization. **Attalla F. El-kott:** Writing – review & editing, Writing – original draft, Visualization, Validation, Supervision, Software, Resources, Project administration, Methodology, Investigation, Formal analysis, Data curation, Conceptualization. **Youssef A. Alqahtani:** Writing – review & editing, Writing – original draft, Visualization, Validation, Supervision, Software, Resources, Project administration, Methodology, Investigation, Funding acquisition, Formal analysis, Data curation, Conceptualization. **Abdullah S. Shatoor:** Writing – review & editing, Writing – original draft, Visualization, Validation, Supervision, Software, Resources, Project administration, Methodology, Investigation, Funding acquisition, Formal analysis, Data curation, Conceptualization. **Mohamed Samir Ahmed Zaki:** Writing – review & editing, Writing – original draft, Visualization, Validation, Supervision, Software, Resources, Project administration, Methodology, Investigation, Funding acquisition, Formal analysis, Data curation, Conceptualization.

Declaration of competing interest

The authors declare the following financial interests/personal relationships which may be considered as potential competing interests:Ayed A. Shati reports financial support was provided by King Khalid University. If there are other authors, they declare that they have no known competing financial interests or personal relationships that could have appeared to influence the work reported in this paper.

Acknowledgements

The authors extend their appreciation to the Deanship of Scientific Research at King Khalid University for funding this work through large group Research Project under grant number RGP2/378/44.

References

[1] K. Fraczkowska, et al., Alterations of biomechanics in cancer and normal cells induced by doxorubicin, Biomed. Pharmacother. 97 (2018) 1195–1203.

[2] P. Prša, et al., The potential use of natural products to negate hepatic, renal and neuronal toxicity induced by cancer therapeutics, Biochem. Pharmacol. 173 (2020) 113551.
[3] K. Renu, et al., Molecular mechanism of doxorubicin-induced cardiomyopathy–An update, Eur. J. Pharmacol. 818 (2018) 241–253.
[4] G. Ibrahim Fouad, K.A. Ahmed, Neuroprotective potential of berberine against doxorubicin-induced toxicity in rat's brain, Neurochem. Res. 46 (12) (2021) 3247–3263.
[5] G. Ibrahim Fouad, K.A. Ahmed, Neuroprotective potential of berberine against doxorubicin-induced toxicity in rat's brain, Neurochem. Res. 46 (12) (2021) 3247–3263.
[6] J.V. McGowan, et al., Anthracycline chemotherapy and cardiotoxicity, Cardiovasc. Drugs Ther. 31 (1) (2017) 63–75.
[7] T. Magdy, B.T. Burmeister, P.W. Burridge, Validating the pharmacogenomics of chemotherapy-induced cardiotoxicity: what is missing? Pharmacol. Therapeut. 168 (2016) 113–125.
[8] K.W. Zhang, et al., Abnormalities in 3-dimensional left ventricular mechanics with anthracycline chemotherapy are associated with systolic and diastolic dysfunction, JACC (J. Am. Coll. Cardiol.): Cardiovascular Imaging 11 (8) (2018) 1059–1068.
[9] C. Galán-Arriola, et al., Serial magnetic resonance imaging to identify early stages of anthracycline-induced cardiotoxicity, J. Am. Coll. Cardiol. 73 (7) (2019) 779–791.
[10] M. Jiang, et al., Mitochondrial metabolism in myocardial remodeling and mechanical unloading: implications for ischemic heart disease, Frontiers in Cardiovascular Medicine 8 (2021) 789267.
[11] F.S. Carvalho, et al., Doxorubicin-induced cardiotoxicity: from bioenergetic failure and cell death to cardiomyopathy, Med. Res. Rev. 34 (1) (2014) 106–135.
[12] M. Sheibani, et al., Doxorubicin-induced cardiotoxicity: an overview on pre-clinical therapeutic approaches, Cardiovasc. Toxicol. 22 (4) (2022) 292–310.
[13] X. Fan, et al., The clinical applications of curcumin: current state and the future, Curr. Pharmaceut. Des. 19 (11) (2013) 2011–2031.
[14] H.S. Mohammed, et al., Protective effect of curcumin nanoparticles against cardiotoxicity induced by doxorubicin in rat, Biochim. Biophys. Acta (BBA) - Mol. Basis Dis. 1866 (5) (2020) 165665.
[15] M. Katamura, et al., Curcumin attenuates doxorubicin-induced cardiotoxicity by inducing autophagy via the regulation of JNK phosphorylation, J. Clin. Exp. Cardiol. 5 (9) (2014) 1–8.
[16] A.V. Swamy, et al., Cardioprotective effect of curcumin against doxorubicin-induced myocardial toxicity in albino rats, Indian J. Pharmacol. 44 (1) (2012) 73.
[17] Carmo de Carvalho, M.d. e Martins, et al., Biological indicators of oxidative stress [Malondialdehyde, catalase, glutathione peroxidase, and superoxide dismutase] and their application in nutrition, in: Biomarkers in Nutrition, Springer, 2022, pp. 1–25.
[18] Y. Sadzuka, et al., Beneficial effects of curcumin on antitumor activity and adverse reactions of doxorubicin, Int. J. Pharm. 432 (1–2) (2012) 42–49.
[19] W. Yu, et al., Curcumin alleviates diabetic cardiomyopathy in experimental diabetic rats, PLoS One 7 (12) (2012) e52013.
[20] X. Lv, et al., Glycyrrhizin improved autophagy flux via HMGB1-dependent Akt/mTOR signaling pathway to prevent Doxorubicin-induced cardiotoxicity, Toxicology 441 (2020) 152508.
[21] Q.-W. Zhang, L.-G. Lin, W.-C. Ye, Techniques for extraction and isolation of natural products: a comprehensive review, Chin. Med. 13 (2018) 1–26.
[22] S. Reitman, S. Frankel, A colorimetric method for the determination of serum glutamic oxalacetic and glutamic pyruvic transaminases, Am. J. Clin. Pathol. 28 (1) (1957) 56–63.
[23] R.A. Greenwald, Handbook Methods for Oxygen Radical Research, CRC press, 2018.
[24] H. Misera, I. Fridovich, The role of superoxide anion in the autooxidation of epinephrine and a simple assay for SOD, J. Biol. Chem. 247 (1972) 3170–3175.
[25] H. Ohkawa, N. Ohishi, K. Yagi, Assay for lipid peroxides in animal tissues by thiobarbituric acid reaction, Anal. Biochem. 95 (2) (1979) 351–358.
[26] I. Martín-Burriel, et al., Histopathological and molecular changes during apoptosis produced by 7H-dibenzo [c, g]-carbazole in mouse liver, Toxicol. Pathol. 32 (2) (2004) 202–211.
[27] U. Würzburg, et al., Quantitative Determination of Creatine Kinase Isoenzyme Catalytic Concentrations in Serum Using Immunological Methods, 1977.
[28] K.S. Suvarna, C. Layton, J.D. Bancroft, Bancroft's Theory and Practice of Histological Techniques E-Book, Elsevier health sciences, 2018.
[29] L.A. Ahmed, et al., Bradykinin-potentiating activity of a gamma-Irradiated bioactive fraction isolated from scorpion (Leiurus quinquestriatus) venom in rats with doxorubicin-induced acute cardiotoxicity: favorable modulation of oxidative stress and inflammatory, fibrogenic and apoptotic pathways, Cardiovasc. Toxicol. 21 (2) (2021) 127–141.
[30] N. Chaffey, M.A. Hayat, Principles and Techniques of Electron Microscopy: Biological Applications, 543pp, fourth ed., Cambridge University Press, Cambridge, 2000, pp. 546–548. £65 (hardback). Annals of Botany, 2001. 87(4).
[31] J. Lam, et al., A universal approach to analyzing transmission electron microscopy with ImageJ, Cells 10 (9) (2021) 2177.
[32] J.H. Doroshow, Effect of anthracycline antibiotics on oxygen radical formation in rat heart, Cancer Res. 43 (2) (1983) 460–472.
[33] S.M. Swain, F.S. Whaley, M.S. Ewer, Congestive heart failure in patients treated with doxorubicin: a retrospective analysis of three trials, Cancer: Interdisciplinary International Journal of the American Cancer Society 97 (11) (2003) 2869–2879.
[34] M. Goudarzi, et al., Protective effect of ellagic acid against sodium arsenite-induced cardio-and hematotoxicity in rats, Cardiovasc. Toxicol. 18 (4) (2018) 337–345.
[35] H. Haybar, et al., Effect of gemfibrozil on cardiotoxicity induced by doxorubicin in male experimental rats, Biomed. Pharmacother. 109 (2019) 530–535.
[36] R. Mete, et al., Protective effects of onion (Allium cepa) extract against doxorubicin-induced hepatotoxicity in rats, Toxicol. Ind. Health 32 (3) (2016) 551–557.
[37] J.M. McCord, I. Fridovich, The utility of superoxide dismutase in studying free radical reactions. I. Radicals generated by the interaction of sulfite, dimethyl sulfoxide, and oxygen, J. Biol. Chem. 244 (22) (1969) 6056–6063.
[38] K.A.D. Sauter, et al., Doxorubicin and daunorubicin induce processing and release of interleukin-1β through activation of the NLRP3 inflammasome, Cancer Biol. Ther. 11 (12) (2011) 1008–1016.
[39] P. Ma, et al., Temporary blockade of interferon-γ ameliorates doxorubicin-induced cardiotoxicity without influencing the anti-tumor effect, Biomed. Pharmacother. 130 (2020) 110587.
[40] H. Zelová, J. Hošek, TNF-α signalling and inflammation: interactions between old acquaintances, Inflamm. Res. 62 (2013) 641–651.
[41] K.A. Conklin, Chemotherapy-associated oxidative stress: impact on chemotherapeutic effectiveness, Integr. Cancer Ther. 3 (4) (2004) 294–300.
[42] A. Iqubal, et al., Molecular mechanism involved in cyclophosphamide-induced cardiotoxicity: old drug with a new vision, Life Sci. 218 (2019) 112–131.
[43] J. Park, et al., A case of successfully treated severe heart failure due to cyclophosphamide induced cardiomyopathy, Clinical Pediatric Hematology-Oncology 25 (2018) 71–75.
[44] D.S. El-Agamy, M.A. Elkablawy, H.M. Abo-Haded, Modulation of cyclophosphamide-induced cardiotoxicity by methyl palmitate, Cancer Chemother. Pharmacol. 79 (2) (2017) 399–409.
[45] Y. Octavia, et al., Doxorubicin-induced cardiomyopathy: from molecular mechanisms to therapeutic strategies, J. Mol. Cell. Cardiol. 52 (6) (2012) 1213–1225.
[46] M.A. Mitry, J.G. Edwards, Doxorubicin induced heart failure: phenotype and molecular mechanisms, Int J Cardiol Heart Vasc 10 (2016) 17–24.
[47] Y. Jiang, et al., Xinmailong attenuates doxorubicin-induced lysosomal dysfunction and oxidative stress in H9c2 cells via HO-1, Oxid. Med. Cell. Longev. 2021 (2021) 5896931.
[48] T.W. LeBaron, et al., A new approach for the prevention and treatment of cardiovascular disorders. Molecular hydrogen significantly reduces the effects of oxidative stress, Molecules 24 (11) (2019).
[49] R.H. Mohamed, R.A. Karam, M.G. Amer, Epicatechin attenuates doxorubicin-induced brain toxicity: critical role of TNF-α, iNOS and NF-κB, Brain Res. Bull. 86 (1–2) (2011) 22–28.
[50] A.L. Has, et al., Olea europaea leaf extract up-regulates Nrf2/ARE/HO-1 signaling and attenuates cyclophosphamide-induced oxidative stress, inflammation and apoptosis in rat kidney, Biomed. Pharmacother. 111 (2019) 676–685.
[51] N. Abdelbaky, A. Ali, M. Raeesa, Cardioprotective effect of simvastatin on doxorubicininduced oxidative cardiotoxicity in rats, J. Basic Appl. Sci. 6 (2010) 29–38.
[52] E. El-Sayed, et al., Cardioprotective effects of Curcuma longa L. extracts against doxorubicin-induced cardiotoxicity in rats, J. Med. Plants Res. 17 (2010).

[53] B.C. Koti, et al., Cardioprotective effect of lipistat against doxorubicin induced myocardial toxicity in albino rats, Indian J. Exp. Biol. 47 (1) (2009) 41–46.
[54] F. Benzer, et al., Curcumin ameliorates doxorubicin-induced cardiotoxicity by abrogation of inflammation, apoptosis, oxidative DNA damage, and protein oxidation in rats, J. Biochem. Mol. Toxicol. 32 (2) (2018).
[55] Y. Chen, et al., Curcumin supplementation improves heat-stress-induced cardiac injury of mice: physiological and molecular mechanisms, J. Nutr. Biochem. 78 (2020) 108331.
[56] S. Nahar, Q.S. Akhter, Effect of Curcuma longa (Turmeric) on serum creatine kinase-MB and troponin I in isoproterenol induced myocardial infarction in wistar albino rats, J. Bangladesh Soc. Physiol. 13 (2) (2018) 47–53.
[57] A.S. Choudhari, et al., Phytochemicals in cancer treatment: from preclinical studies to clinical practice, Front. Pharmacol. 10 (2019) 1614.